Photoresponses in the radiolar eyes of the fan worm, *Acromegalomma vesiculosum* (Montagu)

AUTHORS: Michael J. Bok[1*], Dan-Eric Nilsson[2] & Anders Garm[3]

[1] School of Biological Sciences, University of Bristol, Bristol, BS8 1TQ, UK

[2] Department of Biology, Lund Vision Group, Lund University, Lund, Sweden

[3] Section of Marine Biology, Department of Biology, University of Copenhagen, Denmark

* Corresponding author: mikebok@gmail.com

KEYWORDS: Vision, Electroretinogram, Polychaete, Eyes, Visual Ecology, Fan Worms

SUMMARY STATEMENT: We examine the light responses of unusual eyes on fan worm feeding tentacles, and describe their spectral sensitivity, dynamic range, and temporal resolution in the context of their visual ecology.

ABSTRACT

Fan worms (Annelida: Sabellidae) possess compound eyes and other photoreceptors on their radiolar feeding tentacles. These eyes putatively serve as an alarm system that alerts the worm to encroaching threats, eliciting a rapid defensive retraction into their protective tube. The structure and independent evolutionary derivation of these radiolar eyes make them a fascinating target for exploring the emergence of new sensory systems and visually guided behaviours. However, little is known about their physiology and how this impacts their function. Here we present electroretinogram recordings from the radiolar eyes of the fan worm *Acromegalomma vesiculosum* (Montagu, 1813). We examine their spectral sensitivity along with their dynamic range and temporal resolution. Our results show that they possess one class of photoreceptors with a single visual pigment peaking in the blue-green part of the spectrum around 510 nm, which matches the dominant wavelengths in their shallow coastal habitats. We found the eyes to have a rather high temporal resolution with a critical flicker fusion frequency around 35 Hz. The high temporal resolution of this response is ideally

suited for detecting rapidly moving predators but also necessitates downstream signal processing to filter out caustic wave flicker. This study provides a fundamental understanding of how these eyes function. Furthermore, these findings emphasise a set of dynamic physiological principles that are well-suited for governing a multi-eyed startle response in coastal aquatic habitats.

INTRODUCTION

Radiolar eyes, found on the feeding tentacles of sabellid and serpulid tube worms, are unusual visual sensors (Bok et al., 2016; 2017b). The radiolar tentacles project from the worm's head, up into the water column, leaving the rest of the worm's body within the protective tube (Fig. 1A, B). The radiolar eyes occur in a diversity of arrangements in different species but they are usually widely distributed on the radioles, though some species have a large, consolidated pair. The structural complexity of the eyes varies from scattered single ocelli to compound eyes with hundreds of facets each. Within the Sabellidae and Serpulidae, the radiolar eyes appear to have arisen more than once and have been lost in some taxa (Bok et al., 2016, 2017b). The radiolar eyes are thought to function solely as 'burglar alarms' that respond to shadow threats and initiate a giant-axon-mediated withdrawal response, quickly retracting the worm into its protective tube (Nicol 1948; Nilsson 1994). Behavioural observations have suggested that the withdrawal response is only initiated by a decrease in illumination (Nicol 1950). The wide range in structural complexity of radiolar eyes in the service to a singular behavioural task make them of great interest for exploring the emergence and elaboration of new sensory systems and behaviours, as well as for probing the neural basis of distributed visual processing.

The photoreceptors found in the radiolar eyes are ciliary in nature, with the elaborated sensory membrane formed by stacks of lamellae. Indeed, these were among the first invertebrate ciliary photoreceptors to be identified (Lawrence and Krasne 1965; Krasne and Lawrence 1966). Subsequent fine structure studies of the sabellid genera *Pseudopotamilla* (Kernéis 1971 as *Potamilla*), *Bispira* (Nilsson 1994), and *Branchiomma* (Kerneis 1968; Nilsson 1994; all as *Dasychone*) and a number of serpulid genera (Smith 1984; Bok et al., 2017b), indicated conservation of the ciliary photoreceptor, but revealed significantly different approaches to producing the lenses and pigment cups in each genus. Intracellular recordings have shown that these photoreceptors exhibit a hyperpolarizing response to light

flashes (Leutscher-Hazelhoff, 1984). Transcriptomic analysis has found only invertebrate c-opsins and $G_{i/o}$ g-protein phototransduction cascade components expressed in the radiolar eyes of the sabellid *Acromegalomma interruptum* (Bok et al., 2017a; as *Megalomma interrupta*), and the serpulid *Spirobranchus corniculatus* (Bok et al., 2017b).

The most elaborate radiolar eyes amongst the sabellid fan worms are found in the genus *Acromegalomma* (Gil and Nishi, 2017). Many species of *Acromegalomma* express two large compound eyes on the dorsal-most pair of radioles with varying distributions of smaller compound eyes, apparently composed of the same ommatidia-like ocellar subunits, on some or all of the other more lateral and ventral radioles (Capa and Murray, 2009; as *Megalomma*). In *Acromegalomma*, the eyes are found near the terminus of the radioles. While the radiolar compound eyes of other sabellid genera are composed of fewer than a hundred facets, the dorsal-most radiolar eyes in *Acromegalomma* have hundreds of facets (Capa and Murray, 2009; Bok et al., 2016; both as *Megalomma*). In regard to these facet counts, the sole comparable examples are the bizarre crescent-shaped radiolar compound eyes of the serpulid christmas tree worms, *Spirobranchus corniculatus* (Bok et al., 2017b).

Amongst the sabellids, the visual system of *A. vesiculosum* has received the most attention, with studies on its behavioural light response, photoreceptor fine structure, and intracellular physiological light response (Nicol, 1950; Lawrence and Krasne, 1965; Leutscher-Hazelhoff, 1984; as *Branchiomma vesiculosum* in all). The two large, many-faceted, compound eyes of *A. vesiculosum* are prominently positioned on the dorsal-most radioles, with a broad view of the environment. Therefore, they provide us the potential to explore perhaps the most visually sophisticated and dynamic manifestation of a radiolar eye visual system. *A. vesiculosum* occurs in coastal and estuarine habitats around Western Europe and is abundant in shallow sublittoral and intertidal sand and gravel flats (Ruiz, 2007). Therefore, they are regularly exposed to broad light intensity variations and spectral compositions. In shallow waters, they must also cope with caustic flicker, which involves waves on the surface refracting sunlight in a spatiotemporally varying manner, resulting in rapid, variable intensity fluctuations that pose particular challenges to a visual system (McFarland and Loew, 1983; Maximov 2000; Swirski et al., 2009). In such a light environment, *A. vesiculosum*'s eyes must adapt to constant irregular flicker to avoid withdrawing unnecessarily while still being able to discern potential threats - which are themselves also illuminated with caustic flicker.

A. vesiculosum is an accessible species for experimentation and a promising model to illuminate the functional properties of multi-eye visual systems and startle responses in general. Multi-eyed visual systems are common in marine organisms including echinoderms, bivalves, and jellyfish (Land, 1965; Nilsson et al., 2005; Garm and Nilsson, 2014; Kirwan et al., 2018). This visual approach presents unique challenges and opportunities to their function in aquatic habitats. Compared to paired-cephalic eyes such as ours, distributed eyes must gather and encode light information from many sometimes heavily overlapping nodes in a consistent and interoperable manner. How does such a system adapt to fluctuations in a dynamic light environment in order to reliably communicate salient visual information to the brain? How do many-eyed visual systems compare and relate to other dispersed sensory modalities such as mechanoreception? What visually guided behaviours can be supported by a many-eyed visual system?

Here we employ electroretinogram (ERG) recordings to describe the spectral sensitivity along with the dynamic range and temporal resolution of *A. vesiculosum* eyes. We report that the eyes have a broad dynamic range and that the spectral sensitivity of the eyes indicates a single visual pigment with the wavelength of maximum absorbance (λ_{max}) at 508 nm. Also, we describe an atypical light-off spectral response with asymmetric time-to-peak and consider its possible implications. The critical flicker fusion frequency of the radiolar eyes was a remarkable 35 Hz, indicating high temporal resolution, unusual among many-eyed visual systems. Finally, we present evidence that the smaller lateral eyes have identical light responses to the large dorsal-most eyes, though diminished in amplitude. We consider these physiological properties in the context of the fan worms light environment and their utility in the behavioural response to looming threats. Finally, we explore the properties of the radiolar eyes in comparison to other unorthodox distributed visual systems.

MATERIALS AND METHODS

Animals

Adult specimens of *Acromegalomma vesiculosum* were collected from intertidal sand and gravel flats at low tide on 2 February and 19 April 2018 and at Helford Passage Beach, Cornwall, United Kingdom (50°05'55.5"N 5°07'50.4"W). Collection was conducted with permission and advice from the Helford Marine Conservation Group, Association of Inshore

Fisheries and Conservation Authorities, Natural England, and the Marine Management Organization. Animals were transported to the University of Copenhagen and kept in seawater aquaria at 10°C with a natural light cycle until use. All experiments were conducted within 1 week of collection.

Photography and microscopy

Live *A. vesiculosum* individuals were photographed in aquaria with a Canon 6D Mark II camera with a Canon EF 100mm F/2.8 L USM lens (Canon, Melville, NY). Images of the dissected radiolar eyes were produced by the Canon 6D Mark II with a camera microscope ocular adaptor lens and a 10x objective. The eyes were lit from above from both sides at roughly an angle of 45°. Focal series were captured through the depth of the eye, and then assembled into a focus-stacked image with Zerene Stacker software (Zerene Systems, Richland, WA). Images were processed for brightness, contrast, and colour balance with Adobe Lightroom CC Classic photo editing software (Adobe Systems, San Jose, CA).

Electroretinogram (ERG) setup

ERG measurements were performed according to protocols previously published in Petie et al., (2016). Recordings were amplified 1000 times on a DC1700 differential amplifier (A-M systems Inc., WA, USA), and were filtered with a 50 Hz notch filter, a 0.1 Hz high pass filter, and a 1 kHz low pass filter. The signals were digitised at 1 kHz using a NI USB-6229 DAQ card (National Instruments, TX, USA). The setup was controlled by a custom LabVIEW program (National Instruments, TX, USA). A Luminus CBT-90 LED (Luminus, Sunnyvale, CA, USA) was used for the stimulus. Intensity for v-log-I curves was controlled with neutral density filters in increments of 0.3 or 0.7 log units. Light was transmitted to the eye with a 1 mm light guide ensuring nearly even illumination of the radiolar eye. At full intensity, the light at the exit of the light guide was 2.5×10^2 W sr^{-1} m^{-2}.

Radiolar eye preparations for ERG

Worms were removed from their tubes and the radiolar eyes were retrieved by cutting the radioles just below the eye, above the termination of the ciliated pinnules. The eyes were placed in a room temperature water bath and suction clamped to a glass electrode with an

internal pore diameter of approximately 30 - 40 µm. Cooled water baths were also tested, but there was no appreciable effect on the responses. We attempted various electrode attachment sites on the compound eye surface as well as at the dissected base and the terminal tip of the radiolar tentacle above the eye. All areas produced consistent responses, albeit inverted in polarity for tip and base recordings (Fig. S1A-D) We found that the most stable and highest signal-to-noise ratio responses were obtained from the radiolar tip. Therefore, we focused on tip attachments for the majority of the experiments (Fig. 2A-B). Ablation of the eye from the electrode-coupled radiolar tip completely abolished the light response, showing that the responses originated from the eye photoreceptors and not from some unknown photoreceptor in the radiolar tip.

We compared light-on and light-off responses as well as various adaptation and stimulus durations (Fig. 2C). We found that the best responses for the spectral sensitivity experiments were obtained from dark adapted eyes stimulated with 25 ms flashes. Reliable responses could be achieved with stimuli as brief as 1 ms but only at the highest intensities. 25 ms stimuli were needed to produce consistent impulse responses with dimmer narrow-band spectral stimuli. Light adapted eyes were slower to respond to light-off stimuli, and stimuli below 20 ms were imperceptible, being suppressed by the light-on response at the cessation of the stimulus. Also, light-off responses didn't reach maximum amplitude until around 250 ms or longer. Therefore, for light adapted eyes given light-off stimuli we used a 1 second stimulus duration in spectral sensitivity experiments.

Spectral sensitivity

To assess the spectral response of radiolar eyes we recorded ERG responses to isoquantal spectral stimuli at various wavelengths. This data was then transformed along a v-log-I intensity tuning curve to provide an approximate spectral sensitivity curve without testing multiple intensities at each wavelength.

The eyes were dark adapted for 10 minutes and then stimulated with equal quanta light pulses at 1.7 x 10^{19} photons s^{-1} sr^{-1} m^{-2} at each wavelength. The wavelength was controlled using interference colour filters (half width = 12 nm, CVI Laser, Bensheim, Germany) in steps of 10 or 20 nm between 400 and 680 nm. Equal quanta intensities at each wavelength were set by adjusting the current applied to the stimulus LED and varied from one another by under 5 percent. Spectral sensitivity experiments were conducted by delivering 25 ms stimulus pulses in descending or ascending wavelength order with a 1-

minute interval. A second set of spectral sensitivity measurements were taken by adapting the eye at individual wavelengths of equal intensity (1.7×10^{19} photons s^{-1} sr^{-1} m^{-2}) for 1 minute and then delivering a 1000 ms light-off stimulus. V-log-I series were taken before and after the wavelength recordings using the ND filter sets. The later to make sure that the sensitivity of the eye had not changed during the protocol. In cases where the sensitivity changed over the course of the experiment, usually by increasing in sensitivity, a linear correction was applied to the response dataset.

Analysis

Response data were analysed using Matlab software (version R2017b, The Mathworks, Inc, Natick, Massachusetts). Individual recordings were smoothed using moving average coefficients equal to the reciprocal of the span, with a span of 10 ms for the impulse light-on responses and a span of 50 ms for the broad light-off responses. Examples of raw versus smoothed response data can be seen in Figures 3A and 3B. Response traces were baselined to the average amplitude in the 1 second before the stimulus was initiated. We measured the maximum amplitude in mV and the time-to peak of the response. For spectral sensitivity computations, v-log-I intensity tuning curves were used to transform the response amplitudes (in mV) into relative sensitivity plots by fitting the data to a 3rd order power function (method described in Coates et al., 2006). The plots were normalised, averaged, and fitted with an A1 visual pigment nomogram described in Stavenga et al., (1993).

Critical flicker fusion frequency

Radiolar eyes were light adapted at mid-intensity (1.3×10^{2} W sr^{-1} m^{-2}) for 10 minutes and then presented with a sinusoidal stimulus oscillating between maximum illumination (2.5×10^{2} W sr^{-1} m^{-2}) and dark for 10 Seconds followed by a minute recovery time at average intensity. The oscillation frequency was increased from 5 to 50 Hz in 5 Hz increments for each successive recording. The resulting ERG response recordings were analysed in Matlab. Recordings were then cropped to the length of 25 cycles starting at 5000-ms-post-initiation and fast Fourier transformed (FFT). The response strength was determined as the power of the Fourier transform at the frequency of stimulation. Power curves were generated for each eye at the 10 frequencies and then normalised and averaged. A five percent power threshold was designated as the critical flicker fusion frequency.

RESULTS

Acromegalomma vesiculosum *radiolar eyes*

In *Acromegalomma vesiculosum*, the radiolar eyes are found sub-distally near the medial terminus of the radioles (Fig. 1A-B). A pair of larger, main radiolar eyes are found on the two dorsal-most radioles (Fig. 1C). These eyes bulge out around their axis to provide a nearly spherical field of view (Fig. 1D). Facet counts from these eyes were found to exceed 1,200, the largest yet observed in a single sabellid or serpulid radiolar eye (counts made from unpublished tomography data to appear in a forthcoming publication). *A. vesiculosum* was also found to possess several smaller radiolar eyes of varying sizes near the tips of some of the lateral radioles (Fig. 1E). Below, we report on the ERG response properties of the large main radiolar eyes, followed by a comparison with the smaller lateral eyes.

Light-on and light-off response in radiolar eyes.

The radular eyes display both light-on and light-off responses but with distinct response characteristics (Fig. 2). In dark adapted eyes, light-on stimuli elicited a rapid impulse potential to stimuli as short as 1 ms in duration (Fig. 2C, blue traces). The impulse response peaked 17.0 ± 2.6 ms after stimulus initiation (25 ms stimulus length, maximum intensity stimulus, n = 7). Responses to longer maximum intensity light-on stimuli (typically greater than 30 ms in duration) produced a clear biphasic response, with a slower peak following the initial impulse response (Fig. 2C, blue traces, *(a)*). The amplitude of the secondary peak increased with increasing stimulus duration, and so did the time to peak. All light-on responses ended with a slow light-off response where the amplitude again increased with increasing stimulus duration (Fig. 2C, blue traces, *(c)*).

Light adapted radiolar eyes required a light-off stimulus duration of at least 20 ms to produce a detectable response. When using stimuli with the same change in intensity (increase or decrease respectively) the light-off responses had about twice the amplitude as the light-on responses. The amplitude of the light-off response increased with increasing stimulus duration (Fig. 2C, red traces, *(c)*). The response generally plateaued about 250-ms-post-stimulus, and longer-duration stimuli responses gradually returned to baseline after this point. The off-response peaked on average at 324.7 ± 56.2 ms-post-stimulus-initiation (1000 ms, maximum intensity stimulus, n = 16). For shorter stimuli the response peaked at the end

of the stimulus. After stimulation ended all light-off responses displayed a graded light-on response (Fig. 2C, red traces, *(a)*). This light-on response lacked the secondary peak seen in long duration dark-adapted, light-on stimuli and returned slowly to baseline within a couple of seconds.

Intensity-dependent response properties

Both the light-on and light-off responses showed graded responses to changes in stimulus intensity. Examples of light-on and light-off responses to an intensity series are shown in Fig. 3A and Fig. 3B respectively. Time-to-peak declined with intensity for the light-on responses and was 17.0 ± 2.6 ms at maximum intensity (Fig. 3C). Interestingly, the time-to-peak of the light-off responses became longer with increasing intensity and at maximum intensity it was 324.7 ± 56.2 ms (Fig. 3D). The V-log-I curves from the two responses are close to identical (Fig. 3E) and span at least 3 log units. There was no sign of saturation at the maximum stimulus intensity, strongly suggesting that the dynamic range is even broader.

Temporal resolution of radiolar eyes

Examples of the responses from the radular eyes to sinusoidal stimuli are shown in Fig. 4A. When normalised and cropped to show 25 cycles of the stimulus at various frequencies, the sinusoidal nature of the responses is evident to up to 35 Hz but has disappeared at 40 Hz (Fig. 4B). We estimate the critical fusion frequency of *A. vesiculosum* radiolar eyes to be between 30 and 35 Hz based on the averaged Fourier transform power curves which cross a 5 percent threshold at around 32 Hz (n = 14) (Fig. 4C).

Spectral sensitivity of radiolar eyes

Spectral sensitivity was tested for *A. vesiculosum* radiolar eyes under light-on (Fig. 5A-C) and light-off (Fig. 5D-C) stimulus conditions. Example response recordings at each testing wavelength are shown (Fig. 5A, D). Light-on experiments produced a broad curve with a half width of approximately 100 nm, closely fitting a theoretical opsin curve with λ_{max}= 508 nm (Fig. 5B, n = 7). The spectral curve only deviates from the opsin template between 470 and 490 nm where there is a sharp peak and trough. Light-off experiments

produced a narrow sensitivity curve with a half width of approximately 50 nm, which results in a rather poor best fit to a theoretical opsin curve with λ_{max}= 514 nm (Fig. 5E, n = 14).

We obtained some unusual results in the time-to-peak for the various stimulus wavelengths for the light-off spectral responses. While the light-on responses showed the time-to-peak remaining constant throughout the spectral range (Fig. 5C), light-off spectral responses had an asymmetry in time-to-peak (Fig. 5F). At shorter wavelengths (below 500 nm), responses are at least 100 ms slower than equal amplitude responses at longer wavelengths. This is also evident in the raw response traces shown in Fig. 5D, and in the averaged response amplitude and time-to-peak data displayed in Fig. S2. This pattern is evident in light-off experiments regardless of whether they are exposed to ascending, descending, or randomised wavelength increments of spectral stimuli (not shown).

Lateral radiolar eye photoresponse properties

The experiments with light-off stimuli were repeated with the smaller lateral radiolar eyes. Generally, the lateral eyes produced lower-amplitude responses (average response amplitude to maximum intensity change: 52.7 ± 6.0 mV, n = 6) compared to the dorsal main eyes (98.8 ± 27.2 mV, n = 16). However, all other response properties were consistent with the results from the main radular eyes (Fig. 6). The light-off response of the lateral eyes peaked at 390.8 ± 81.1 ms-post-stimulus-initiation (1000 ms, maximum intensity stimulus, n = 6). The v-log-I curves from the lateral radular eyes did not saturate either and closely matched those of the dorsal eyes (Fig. 6A). Their critical flicker fusion curve was comparable to the dorsal eyes, with a threshold above the background noise around 25 to 30 Hz (n = 7) (Fig. 6B). The light-off spectral sensitivity curve of the lateral radular eyes also closely resembled that of the dorsal eyes; with a narrow curve again resulting in a poor bestfit to a theoretical opsin template with λ_{max}= 510 nm (n = 6) (Fig. 6C).

DISCUSSION

In this study, we explored the photoresponse properties of the radiolar eyes of a fan worm, *Acromegalomma vesiculosum,* in order to better understand the function of this unusual visual system. We found that the radiolar eyes have a high temporal resolution, broad-dynamic range, and are maximally sensitive to blue-green light, making them well suited for their presumed role as a looming threat detector for a stationary, many-eyed animal

in a shallow marine habitat. Furthermore, photoresponses were similar between the large main eyes and smaller lateral eyes, suggesting that they are formed from similar photoreceptors and function analogously. These findings offer a number of considerations regarding the function and evolution of the radiolar eyes and other unorthodox visual systems.

Functional properties of A. vesiculosum *radiolar eyes*

Our spectral response experiments indicated the presence of a single photoreceptor type with a λ_{max} of 508 nm and a sensitivity curve closely fitting the alpha absorbance band of an A1 visual pigment (Stavenga et al., 1993). However, it should be noted that we did not test for responses at wavelengths below 400 nm and thus cannot rule out the presence of an additional ultraviolet receptor. The maximum spectral response of the *A. vesiculosum* radiolar eyes matches the dominant wavelengths in their coastal or estuarine habitats, where peak downwelling irradiance can vary between 490 and 580 nm depending on turbidity from runoff or phytoplankton blooms (Jerlov, 1976; Baker and Smith, 1982; Cheroske and Cronin, 2005). Matching the λ_{max} of a visual pigment to the wavelength of the maximum irradiance in the water allows animals to optimally detect silhouettes against a predominant uniform backlight (Lythgoe, 1998; Lythgoe and Partridge, 1989).

The temporal resolution of the radiolar eyes is high, between 30-35 Hz at a minimum. Since measurement of critical flicker fusion frequency is dependent on intensity, the radiolar eye temporal resolution could be even faster if tested with a higher intensity stimulus. This high temporal resolution allows the worms to detect rapidly approaching threats, and also to putatively resolve finer movement properties of a stimulus. Nicol (1950) noted that the *A. vesiculosum* withdrawal response was stronger and more resistant to adaptation when the shadow stimuli were moving. It could be that these fan worms are able to assess whether objects are moving towards them or not, and thus avoid withdrawing unnecessarily.

The radiolar eyes respond over a broad intensity range spanning at least 3 log units and the responses did not saturate at the maximum intensity of our stimulus (2.5×10^2 W sr^{-1} m^{-2}). Solar irradiance at sea level at noon on a clear day is about 1.0×10^3 W m^{-2}, and it is likely that the radiolar eyes remain fully responsive at that intensity. Furthermore, the radiolar eyes can function throughout daylight and sunset hours, when visual predators are most active, until near civil twilight (approximately 1 W m^{-2}) (Cronin et al., 2014). However, the radiolar eyes would not be responsive to stimuli in moon or starlight. Supporting this, we

have observed that *A. vesiculosum* does not respond to visual stimuli in the dark, or for a time after the lights have been turned on in their aquaria facilities (unpublished observations).

Tuning of radiolar eye light responses

It has been previously reported that *A. vesiculosum,* and other sabellids and serpulids, only respond behaviourally to decreases in light intensity (Nicol 1950; Smith, 1985). Therefore, we were interested in examining the ERG responses of these eyes in a behaviourally relevant context; light-adapted, off-stimuli experiments. Light-off stimuli elicited a greater-amplitude average response than light-on stimuli but reached their response maximum slower. Also, light-off stimuli needed to be sustained longer than light-on stimuli in order to illicit a response. This could indicate a low-pass temporal filtering effect specific to the off-response in the photoreceptors.

Our results also offer some considerations regarding the processing of visual stimuli downstream of the eyes in the central nervous system. Nicol (1950) found that *A. vesiculosum* exhibited adaptation to repeated light-dimming stimuli presented to the worms at intervals of 1-10 minutes. We did not observe any instances of adaptation in the responses of the radiolar eyes to repeated photo-stimulations of light-on or -off stimuli at such time intervals, suggesting that the habituation mechanism is located downstream of the radiolar eyes in the central nervous system. Similarly, since the radiolar eyes respond to both on and off photic stimuli, albeit with different response dynamics, it strongly suggests that the behavioural decision to only withdraw with decreases in light is also made downstream of the eyes. Furthermore, intracellular recordings from Leutscher-Hazelhoff (1984) found that *A. vesiculosum* (as *Branchiomma*) radiolar eye photoreceptors hyperpolarise in response to a light-on stimulus. Therefore, depolarization of these photoreceptors is seemingly necessary to initiate a downstream withdrawal response by the brain.

The spectral off-response curve is perplexing. Whereas the light-on spectral curve nicely fits a visual pigment template and has a consistent time-to-peak throughout the response range, the off spectral curve is very narrow, and the time-to-peak is asymmetric across the spectral response range. We could not find other examples of electroretinography displaying this phenomenon. A possible explanation would be the presence of two types of photoreceptors in the eyes, with one sensitive to shorter wavelengths and producing an inhibitory response that narrows the overall sensitivity range or possessing alternate phototransduction cascade components causing the asymmetrical response times. The on

response has a small secondary sensitivity peak at 470 nm, the same area of the spectrum that is suppressed in the off-response spectral curve. This could be an indication of an additional photoreceptor active at these wavelengths. However, in the related species *Acromegalomma interruptum*, transcriptomic sequencing has only detected a single expressed opsin in the radiolar eyes (Bok et al., 2017a; as *Megalomma interrupta*). Alternatively, chromatic optical filtering pigments could be used to diversify photoreceptor spectral sensitivities (Douglas and Marshall, 1999; Bok et al., 2014). Beyond a second photoreceptor type in the radiolar eyes, there are a few other possible explanations for the off spectral response. For one, there could be some adaptation mechanism within the photoreceptors that is enhancing the sensitivity in the centre of the response curve when eyes are light adapted. Alternatively, the photoreceptors could contain a sensitising pigment akin to those in many flies (Kirschfeld and Franceschini, 1977). Sensitising pigments absorb light and transfer that energy to visual pigments, augmenting their sensitivity. The secondary sensitivity peak in the on response at 470 nm could be caused by a sensitising pigment that also affects the off response in some manner. Further investigation is required in order to adequately explain these observations.

Visual capabilities of fan worm radiolar eyes

Many questions remain regarding the fan worm radiolar eyes. Are these eyes capable of visual tasks beyond simple shadow detection, such as low-resolution vision (Nilsson, 2013; Nilsson and Bok, 2017)? Certainly, the majority of sabellids and serpulids seemingly lack the compound eye organizational sophistication required for image-forming vision (Bok et al., 2016; 2017b), though recent work on sea urchins suggests that complex eyes are not necessarily required for coarse spatial vision tasks (Kirwan et al., 2018). However, species of *Acromegalomma*, as well as the serpulid Christmas tree worm, *Spirobranchus corniculatus*, have large, consolidated eyes with over 1000 facets each. It remains to be seen if information from these eyes is processed in such a way as to produce a spatial representation of the world that could provide these species with more finely tuned responses to specific threats. Spatial sensitivity to moving or looming stimuli would be a valuable visual asset to these animals; allowing them to avoid false alarms in dynamic light environments that waste energy and truncate their feeding and respiration activities. Their behavioural response thresholds to various visual stimuli need to be rigorously compared between species with consolidated versus distributed radiolar eye arrangements. This will determine if large consolidated

compound eyes such as those in *Acromegalomma* provide functional benefits beyond a more economic organisation of optical, neurological and metabolic resources.

Photoresponses of many-eyed visual systems

The fan worm radiolar eyes can be compared to other unorthodox many-eyed visual systems. These sensory systems present unique visual challenges when compared to the consolidated, paired-cephalic-eyed visual systems found in most animals. Many-eyed or distributed visual systems and the behaviours they control have been described in jellyfish (Nilsson et al 2005, Garm et al., 2007a), starfish (Garm and Nilsson, 2014; Petie et al., 2016a) sea urchins (Kirwan et al., 2018), scallops (Land, 1965; Speiser and Johnsen, 2008), arc clams (Nilsson, 1994), and chitons (Kingston et al., 2018). These visual systems have typically been implicated in phototactic orientation, navigation and obstacle avoidance, or shadow-response behavioural tasks. However, in some cases it is hypothesised that these eyes are capable of more sophisticated visual tasks.

Electroretinography has been performed on the visual systems of box jellies (Garm et al., 2007b; O'Connor et al., 2010; Garm et al., 2016), starfish (Garm and Nilsson, 2014; Petie et al., 2016b), and scallops (Wald and Seldin, 1968; Kanmizutaru et al., 2005). As in the fan worms, other simple or many-eyed visual systems often have spectral responses that match the dominant downwelling light in the habitat. However, the fan worm radiolar eyes are apparently unique in that they have a rather high temporal resolution as measured by critical flicker fusion frequency (30-35 Hz) compared to other simple visual systems. This is unsurprising in the case of slow-moving animals that use these eyes for orientation, often in relation to large, stationary cues, such as in box jellyfish (2.5 Hz in *Copula sivickisi* and 8-10 Hz in *Tripedalia cystophora*; Garm et al., 2007b; O'Connor et al., 2010; Garm et al., 2016) and starfish (0.6-0.7 Hz in *Acanthaster planci*; Petie et al., 2016b). However, this is also the case when compared to other eyes that govern a startle response, such as in scallops (1.3 to 1.5 Hz; Wald and Seldin, 1968; Kanmizutaru et al., 2005), though these eyes may also be involved in orientation towards grassbeds (Hamilton and Koch, 1996). It could be that these other creatures rely on low-pass filtering of temporal stimulation by the eye in order to filter out high frequency wave flicker and improve object detection (McFarland and Loew, 1983; Maximov, 2000), while the fan worms have opted to address this with adaptive neural processing. This would allow the fan worms to remain sensitive to rapidly moving threats but would demand a greater neural investment.

It is also crucial to determine how visual information is processed in the fan worm brain. The synaptic terminals for the photoreceptors must be identified. The fan worm startle response is transmitted to muscles in the body via a giant axon system (Nicol 1948). These giant axons originate in the supraesophageal ganglion of the brain. The withdrawal response can also be rapidly initiated via mechanical stimulation of the radiolar crown (Krasne, 1965), and also makes use of the giant axon pathway (Nicol, 1951). Do mechanosensors and photoreceptors synapse in the same areas adjacent to the giant axons? Are these different sensory modalities using the same neural pathways, and could one have developed from the other? Answering these questions can provide clues regarding the origin and surprising flexibility of the radiolar eyes in fan worms.

Beyond the sabellids and serpulids, a number of other polychaetes display a shadow response, including sabellariids, which employ a similar tube-dwelling lifestyle, as well as the semi-errant *Platynereis dumerilii*. Interestingly, all of these shadow response systems seem to be mediated by different photoreceptor systems: C-opsins in ciliary photoreceptors in sabellids and serpulids (Bok et al., 2017a,b), rhabdomeric photoreceptors with unknown opsins in sabellariids (Meyer et al., 2018; Helm et al., 2018), and a tetraopsin in unknown cirral photoreceptors of *P. dumerilii* (Ayers et al., 2018). Did all of these shadow responses evolve independently and do they all feed into a similar giant axon startle response pathway?

Finally, there are exciting questions regarding the development of fan worm radiolar eyes. Here we showed that the smaller, lateral radiolar eyes had generally similar response properties to the dorsal main eyes and are presumably composed of identical photoreceptor and optical elements in smaller numbers. What factors drive the elaboration of these eyes to the different levels of sophistication seen in *A. vesiculosum*, and the even more widely variable arrangements seen across other species of fan worms? Indeed, fan worms offer unique opportunities to study the evolution and elaboration of sensory systems.

ACKNOWLEDGEMENTS

We would like to thank David Fenwick Snr. for assistance in collecting fan worms as well as Sue Scott from the Helford Voluntary Marine Conservation Group for oversight of animal collection. We also thank Sophie Banham at the Plymouth Marine Biological Association and Chris Lowe at the University of Exeter, Penryn Campus for use of aquaria during collection. We thank Nicholas Roberts, Martin How, and Eric Warrant for enlightening discussions about the work.

COMPETING INTERESTS

No competing interests declared

FUNDING

This work was supported by the UK Research and Innovation: Biotechnology and Biological Sciences Research Council (grant BB/P011357/1) and the Swedish Science Research Council (grant 2015-04690).

AUTHOR CONTRIBUTIONS

MJB designed the project, carried out the experiments, analysed the data, and edited the manuscript. ALG assisted with the experimental design, data analysis, and in editing the manuscript. D-EN assisted with experimental design and edited the manuscript.

REFERENCES

Ayers, T., Tsukamoto, H., Gühmann, M., Veedin Rajan, V. B. and Tessmar-Raible, K. (2018). A Go-type opsin mediates the shadow reflex in the annelid *Platynereis dumerilii*. *BMC Biol.* **16**, 41–9.

Baker, K. S. & Smith, R. C. (1982). Bio-optical classification and model of natural waters. II. *Limnol. Oceanogr.* **27**, 500-509.

Bok, M. J., Porter, M. L., Place, A. R. and Cronin, T. W. (2014). Biological sunscreens tune polychromatic ultraviolet vision in mantis shrimp. *Curr. Biol.* **24**, 1636–1642.

Bok, M. J., M. Capa and D.-E. Nilsson. (2016). Here, There and Everywhere: The Radiolar Eyes of Fan Worms (Annelida, Sabellidae). *Int. Comp. Biol.* **56**, 784-795

Bok, M. J., M. L. Porter and D.-E. Nilsson. (2017a). Phototransduction in Fan Worm Radiolar Eyes. *Curr. Biol.* **27**, R698 - R699.

Bok, M. J., R. Smith, M. L. Porter, H. A. ten Hove and D.-E. Nilsson. (2017b). The radiolar eyes of serpulid fan worms (Annelida, Serpulidae). *Biol. Bull.* **233**, 39-57.

Capa, M. and Murray, A. (2009). Review of the genus *Megalomma* (Polychaeta: Sabellidae) in Australia with description of three new species, new records and notes on certain features with phylogenetic implications. *Rec. Aust. Mus.* **61**, 201–224.

Cheroske, A. G. and Cronin, T. W. (2005). Variation in Stomatopod (*Gonodactylus smithii*) Color Signal Design Associated with Organismal Condition and Depth. *Brain Behav. Evol.* **66**, 99–113.

Coates, M. M., Garm, A., Theobald, J. C., Thompson, S. H. and Nilsson, D.-E. (2006). The spectral sensitivity of the lens eyes of a box jellyfish, *Tripedalia cystophora* (Conant). *J. Exp. Biol.* **209**, 3758–3765.

Cronin, T. W., Johnsen, S., Marshall, N. J. and Warrant, E. J. (2014). *Visual Ecology*. Princeton University Press.

Douglas, R. H. and Marshall, N. J. (1999). A review of vertebrate and invertebrate ocular filters. In *Adaptive mechanisms in the ecology of vision* (eds. Archer, S., Djamgoz, M. B., Loew, E. R., Partridge, J. C., and Vallerga, S., pp. 95–162. Dordrecht: Springer Netherlands.

Garm, A. and Nilsson, D.-E. (2014). Visual navigation in starfish: first evidence for the use of vision and eyes in starfish. *Proc. R. Soc. B.* **281**: 20133011.

Garm, A., O'Connor, M., Parkefelt, L. and Nilsson, D.-E. (2007a). Visually guided obstacle avoidance in the box jellyfish *Tripedalia cystophora* and *Chiropsella bronzie*. *J. Exp. Biol.* **210**, 3616-3623.

Garm, A., Coates, M. M., Gad, R., Seymour, J. and Nilsson, D.-E. (2007b). The lens eyes of the box jellyfish *Tripedalia cystophora* and *Chiropsalmus sp*. are slow and color-blind. *J. Comp. Physiol. A* **193**, 547–557.

Garm, A., Bielecki, J., Petie, R. and Nilsson, D.-E. (2016). Hunting in Bioluminescent Light: Vision in the Nocturnal Box Jellyfish *Copula sivickisi*. *Front. Physiol.* **7**, 634–9.

Gil, J. and Nishi, E. (2017). Nomenclatural checklist for *Acromegalomma* species (Annelida, Sabellidae), a *nomen novum* replacement for the junior homonym *Megalomma* Johansson, 1926. *ZooKeys* **677**, 131–150.

Hamilton, P. V. and Koch, K. M. (1996). Orientation toward natural and artificial grassbeds by swimming bay scallops, *Argopecten irradians* (Lamarck, 1819). *J. Exp. Mar. Biol. Ecol.* **199**, 79–88.

Helm, C., Bok, M. J., Hutchings, P., Kupriyanova, E. and Capa, M. (2018). Developmental studies provide new insights into the evolution of sense organs in Sabellariidae (Annelida). *BMC Evol. Biol*. **18**, 149.

Jerlov, N. G. (1976). *Marine Optics*, Elsevier Science Publishing Company, New York.

Kanmizutaru, T., Anraku, K. and Toyoda, S. (2005). Light perception capability of pallial eyes in Japanese moon scallop *Amusium japonicum* as determined by electroretinogram. *Nippon Suisan Gakkaishi* **71**, 928-934.

Kernéis, A. (1966). Photorécepteurs du panache de *Dasychone bombyx* (Dalyell) Annélides Polychétes. *C. R. Acad. Sci.* **263**, 653–6.

Kernéis, A. (1971). Etudes histologique et ultrastructurale des organes photorécepteurs du panache de *Potamilla reniformis* (OF Müller), Annélide Polychéte. *C. R. Acad. Sci.* **273**, 372–5.

Kingston, A. C. N., Chappell, D. R. and Speiser, D. I. (2018). Evidence for spatial vision in *Chiton tuberculatus*, a chiton with eyespots. *J. Exp. Biol.* **221**, jeb183632

Kirschfeld, K. and Franceschini, N. (1977). Evidence for a sensitising pigment in fly photoreceptors. *Nature*, **269**, 386–390.

Kirwan, J. D., Bok, M. J., Smolka, J., Foster, J. J., Hernández, J. C. and Nilsson, D.-E. (2018). The sea urchin *Diadema africanum* uses low resolution vision to find shelter and deter enemies. *J. Exp. Biol.* **221**, jeb176271.

Krasne, F. B. (1965). Escape from recurring tactile stimulation in *Branchiomma vesiculosum. J. Exp. Biol.* **42**, 307-322.

Krasne, F. B. and Lawrence, P. A. (1966). Structure of the Photoreceptors in the Compound Eyespots of *Branchiomma vesiculosum*. *J. Cell Sci.* **1**, 239–248.

Land, M. F. (1965). Image formation by a concave reflector in the eye of the scallop, *Pecten maximus*. *J. of Physiol.* **179**, 138–153.

Lawrence, P. A. and Krasne, F. B. (1965). Annelid Ciliary Photoreceptors. *Science* **148**, 965–966.

Leutscher-Hazelhoff, J. T. (1984). Ciliary cells evolved for vision hyperpolarize—Why? *Naturwissenschaften* **71**, 213–214.

Lythgoe, J.N., (1988). Light and vision in the aquatic environment. In *Sensory biology of aquatic animals* (pp. 57-82). Springer, New York, NY.

Lythgoe, J.N. and Partridge, J.C. (1989). Visual pigments and the acquisition of visual information. *J. Exp. Biol.* **146**, 1-20.

Maximov, V. V. (2000). Environmental factors which may have led to the appearance of colour vision.*Philos. Trans. Royal Soc. B* **355**, 1239–1242.

McFarland, W. N. and Loew, E. R. (1983). Wave produced changes in underwater light and their relations to vision. *Environ. Biol. Fishes* **8**, 173–184.

Meyer, C., Faroni-Perez, L. and Purschke, G. (2018). Anterior sense organs in *Sabellaria alveolata* (Annelida, Sedentaria, Spionida) with special reference to ultrastructure of photoreceptor elements presumably involved in shadow reflex. *Zoomorphology* **138**, 39–54.

Montagu, G. (1813). Descriptions of several new or rare animals, principally marine, discovered on the south coast of Devonshire. *Trans. Linn. Soc. Lond.* **11**, 1–26.

Nilsson, D.-E. (1994). Eyes as optical alarm systems in fan worms and ark clams. *Philos. Trans. Royal Soc. B* **346**, 195–212.

Nilsson, D.-E. (2013). Eye evolution and its functional basis. *Vis. Neurosci.* **30**, 5–20.

Nilsson, D.-E. and M.J. Bok. (2017). Low-resolution vision – at the hub of eye evolution. *Int. Comp. Biol.* **57**, 1066–1070.

Nilsson, D.-E., Gislén, L., Coates, M. M., Skogh, C. and Garm, A. (2005). Advanced optics in a jellyfish eye. *Nature* **435**, 201–205.

Nicol, J. A. C. (1948). The giant axons of annelids. *Q. Rev. Biol.* **23**, 291–323.

Nicol, J. A. C. (1950). Responses of *Branchiomma vesiculosum* (Montagu) to photic stimulation. *J. Mar. Biol. Assoc.* **29**, 303–320.

Nicol, J. A. C. (1951). Giant axons and synergic contractions in *Branchiomma vesiculosum*. *J. Exp. Biol.* **28**, 22–31.

O'Connor, M., Nilsson, D.-E. and Garm, A. (2010). Temporal properties of the lens eyes of the box jellyfish *Tripedalia cystophora*. *J. Comp. Physiol. A* **196**, 213–220.

Petie, R., Garm, A. and Hall, M. R. (2016a). Crown-of-thorns starfish have true image forming vision. *Front. Zool.* **13**, 41.

Petie, R., Hall, M. R., Hyldahl, M. and Garm, A. (2016b). Visual orientation by the crown-of-thorns starfish (*Acanthaster planci*). *Coral Reefs* **35**, 1139–1150.

Ruiz, A. (2007). *Acromegalomma vesiculosum* A fanworm. In Tyler-Walters H. and Hiscock K. (eds) *Marine Life Information Network: Biology and Sensitivity Key Information Reviews,* [on-line]. Plymouth: Marine Biological Association of the United Kingdom. [cited 24-10-2019]. Available from: https://www.marlin.ac.uk/species/detail/2167

Smith, R. S. (1984). Novel organelle associations in photoreceptors of a serpulid polychaete worm. *Tissue & Cell* **16**, 951–956.

Smith, R. S. (1985). Photoreceptors of Serpulid Polychaetes. Ph.D. dissertation, James Cook University, Townsville, Australia.

Speiser, D. I. and Johnsen, S. (2008). Scallops visually respond to the size and speed of virtual particles. *J. Exp. Biol.* **211**, 2066–2070.

Stavenga, D. G., R. P. Smits, and Hoenders, B. J. (1993) Simple exponential functions describing the absorbance bands of visual pigment spectra. *Vision Res.* **33**, 1011–1017.

Swirski, Y., Schechner, Y. Y., Ben Herzberg and Negahdaripour, S. (2009). Stereo from flickering caustics. *2009 IEEE 12th International Conference on Computer Vision* 205–212.

Wald, G. and Seldin, E. B. (1968). Electroretinogram and spectral sensitivity of the common scallop. *Biol. Bull.* **135**, 441-422.

Figures

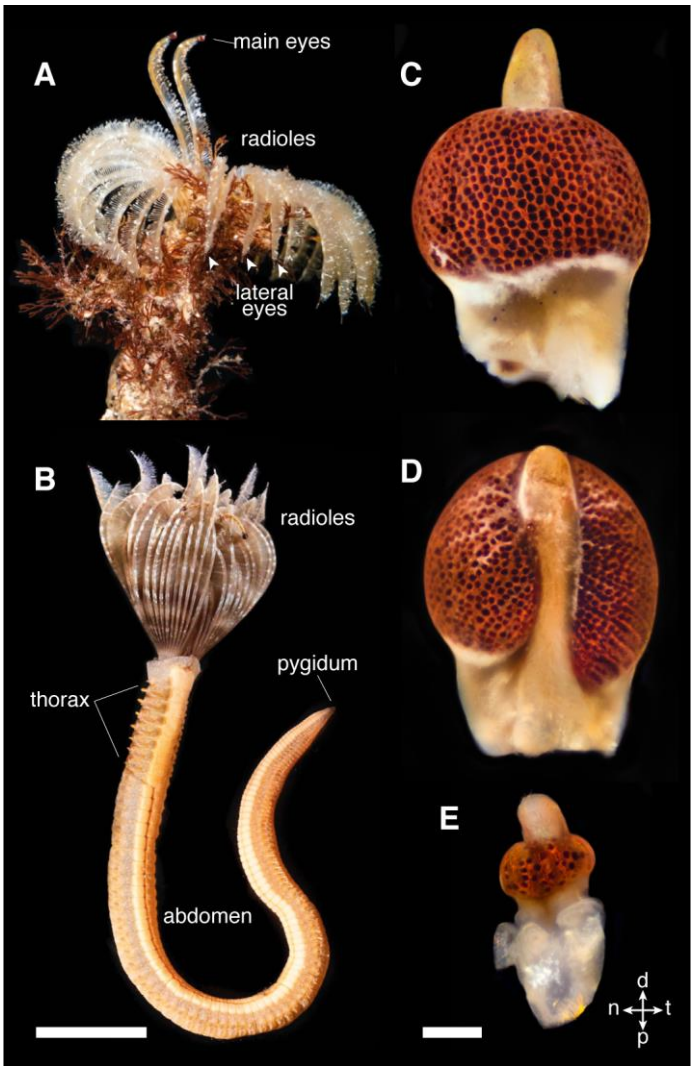

FIGURE 1. The radiolar eyes of *Acromegalomma vesiculosum*. (A) *A. vesiculosum* projecting its radiolar fan up out of its tube. The two main eyes are prominently positioned, and the positions of some lateral eyes are indicated with arrowheads. **(B)** An *A. vesiculosum* individual removed from its tube. **(C-E)** Radiolar eyes from *A. vesiculosum*. A large, main eye is shown front (C) and back (D), as well as the frontal view of a smaller lateral eye (E). Scale bars: B, 5 mm; C-D, 100 μm. Orientation for all eye micrographs is shown below E: (d)istal, (p)roximal, (n)asal, (t)emporal.

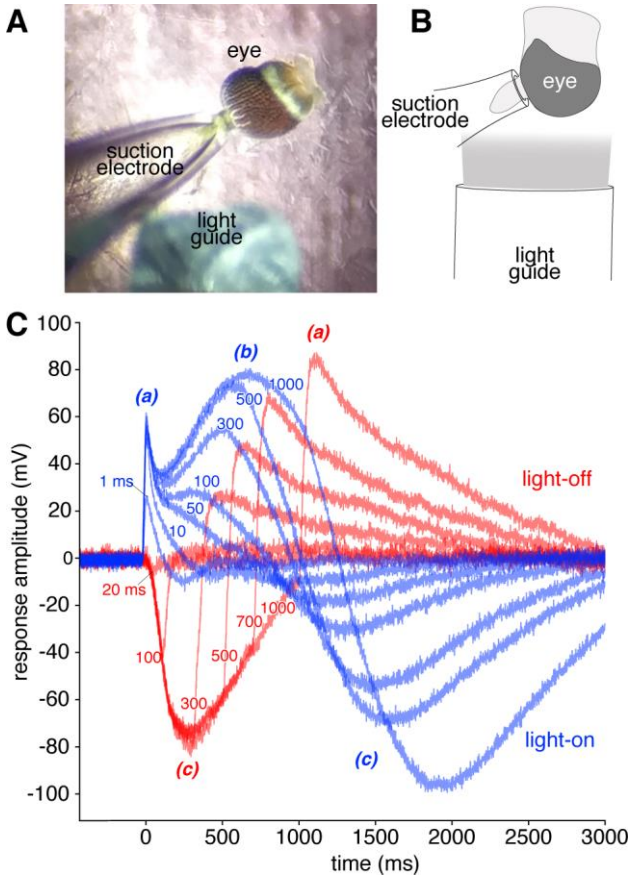

FIGURE 2. ERG responses from the radiolar eyes of *Acromegalomma vesiculosum*. (A-B) A micrograph (**A**) and diagram (**B**) of the ERG preparation used in these experiments. Eyes were suction-clamped via the radiolar tip, producing stronger, more reliable response recordings than attachment to the eye surface (Fig. S1). **(C)** ERG response recordings from *A. vesiculosum* radiolar eyes with increasing stimulus durations (indicated by labels on the plot in ms), and using two different stimuli; Light-on (blue traces), and light-off (red traces). Labels in italics indicate the prominent features of the light response: *(a)*, light-on impulse; *(b)*, light-on secondary response; *(c)*, light-off response. Minimum detectable impulse responses are shown for light-on (1 ms stimulus, the minimum duration in our setup), and light-off stimuli (approximately 20 ms stimulus).

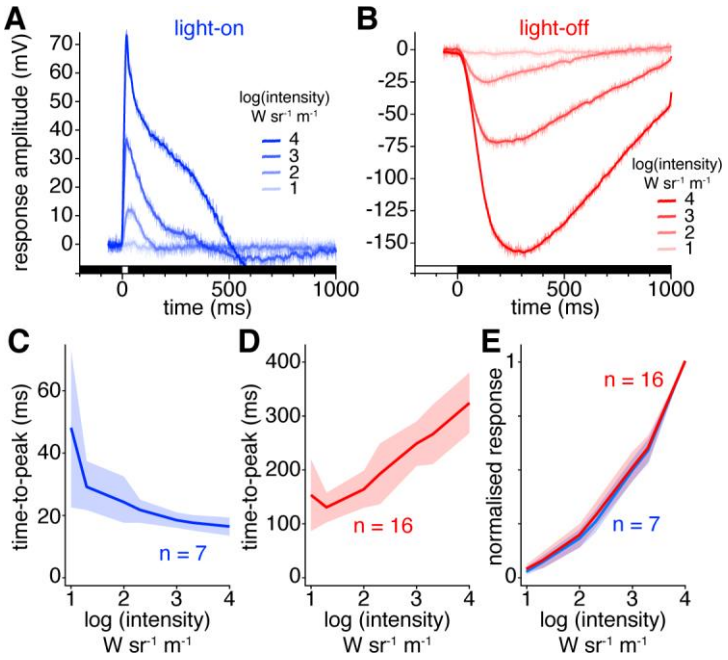

FIGURE 3. ERG responses from the radiolar eyes of *Acromegalomma vesiculosum* under increasing intensities of light-on (A) and light-off stimuli (B). Example ERG recordings showing the response properties of the *A. vesiculosum* radiolar eyes to stimuli of varying intensities (indicated by trace opacity). Raw data are overlaid with smoothed traces. Stimulus duration was 25 ms for light-on and 1000 ms for light-off stimuli. **(C-D)** Plots showing average time to peak in ms ± SD for light-on (C, blue) and light-off (D, red) stimuli. **(E)** Average V-log-I curves with responses normalised ± SD for light-on (blue) and light-off (red) stimuli.

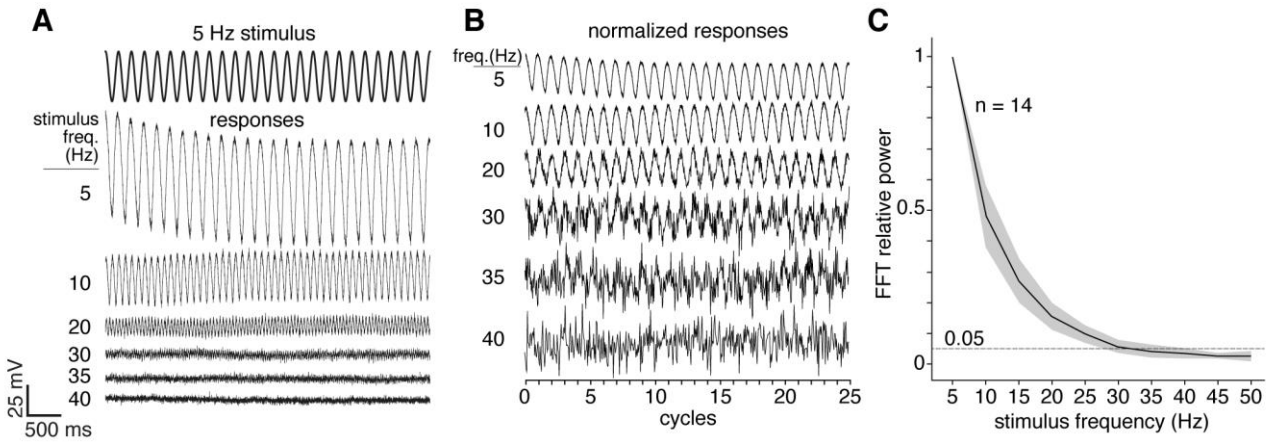

FIGURE 4. Critical flicker fusion frequency in *Acromegalomma vesiculosum* radiolar eyes. (A) Example 5 second recordings (black traces) from an *A. vesiculosum* eye in response to a sinusoidal flickering light stimulus of increasing frequencies. A 5 Hz example stimulus in shown in bold. **(B)** Normalised flicker recordings from tested frequencies expanded to show the time range for 25 cycles of each of the stimulus frequencies. These are the data that were analysed by FFT to determine critical flicker fusion frequency thresholds. Note that the sine wave pattern is discernible to 35 Hz in this example. **(C)** A plot showing the average relative FFT power of main eye flicker responses (n = 14). Grey shading indicates SD.

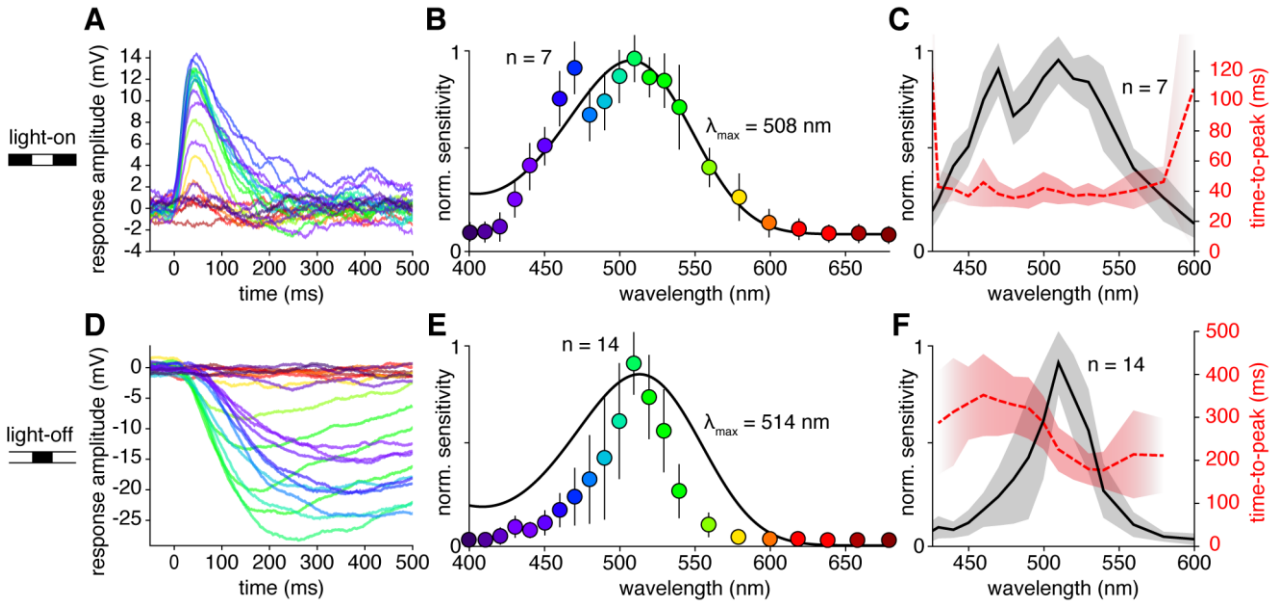

FIGURE 5. Spectral sensitivity in *Acromegalomma vesiculosum* radiolar eyes in response to light-on (A-C) and light-off stimuli (D-F). (A, D) Example recordings with trace colour indicating human colour perception of stimulus wavelength. **(B, E)** Averaged spectral sensitivity curves (circles indicating wavelength colour, ± SD), and visual pigment best fit templates (black lines). **(C, F)** Spectral sensitivity curves (black lines ± SD) plotted against the average time-to-peak at each tested wavelength (red dashed lines ± SD).

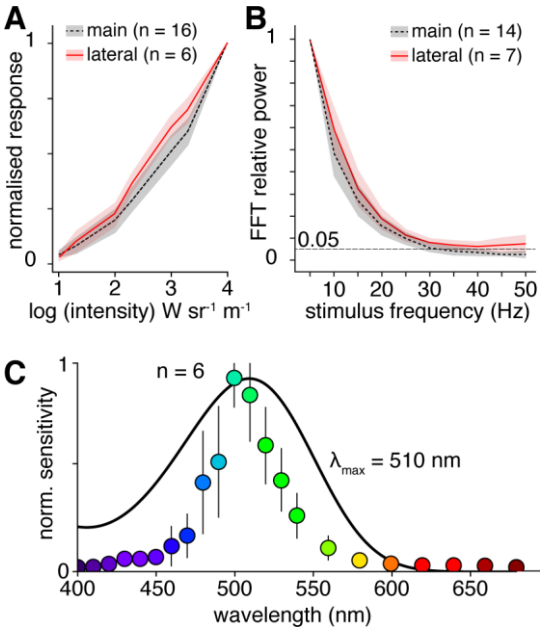

FIGURE 6. ***Acromegalomma vesiculosum*** **lateral eye ERG response properties. (A)** Averaged V-log-I curves for main radiolar eyes (dashed black line) and lateral radiolar eyes (red line). **(B)** Averaged critical flicker fusion frequency FFT power curves for main (dashed black line) and lateral eyes (red line). **(C)** Averaged light-off spectral sensitivity curve for lateral radiolar eyes (circles indicating wavelength colour, ± SD) overlaid with a best fit visual pigment nomogram (black line).

SUPPLEMENTAL MATERIALS for

Photoresponses in the radiolar eyes of the fan worm, *Acromegalomma vesiculosum* (Montagu)

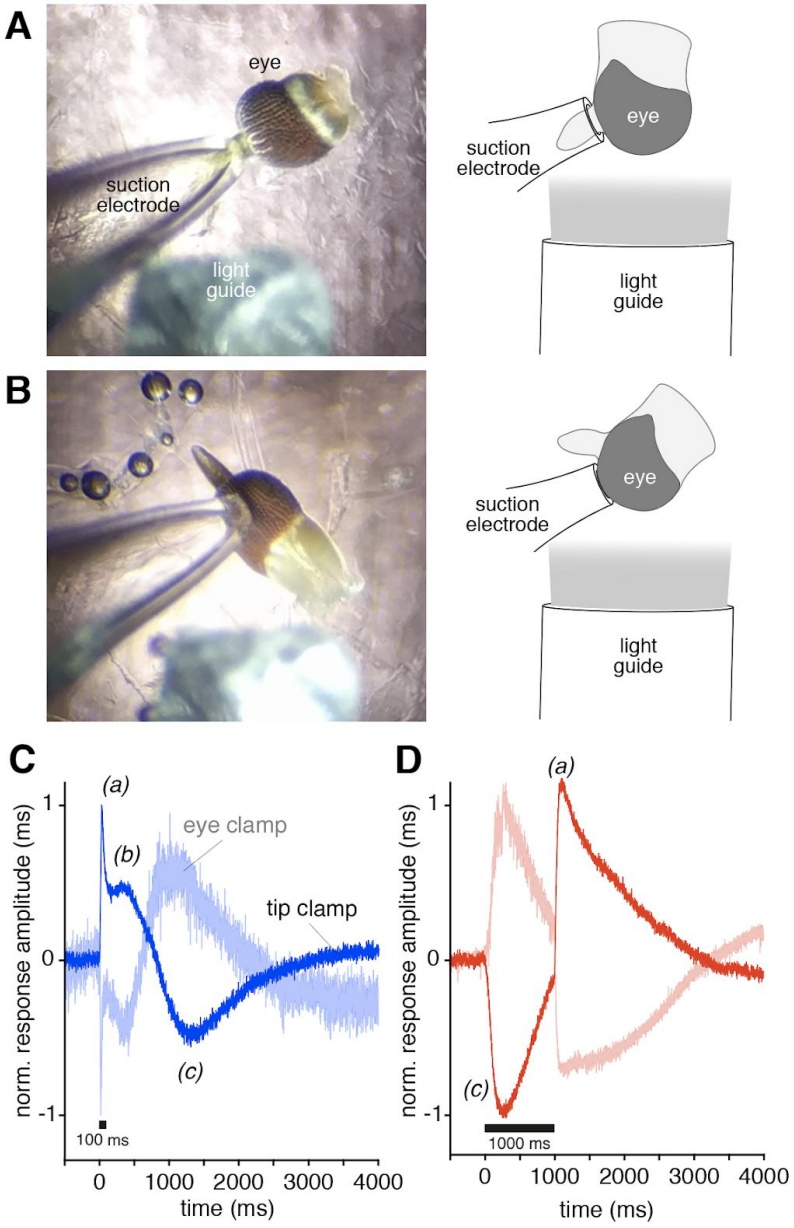

FIGURE S1. (A-B) Micrographs and diagrams of the two ERG preparations used in these experiments; tip suction clamped (A) and eye suction clamped (B). **(C-D)** ERG recordings (in mV, normalised to initial response amplitude) from *A. vesiculosum* radiolar eyes under eye-clamped (light trace) and tip-clamped (dark trace) preparations. Responses are shown for light-on (C, blue traces) and light-off (D, red traces) stimuli. Stimulus durations are indicated by black bars below the traces. Panels C and D include labels for the primary components of the light response: *(a),* light-on primary response; *(b)*, light-on secondary response; *(c),* light-off response. Eyes that were suction-clamped via the radiolar tip produced stronger and more reliable responses but were comparable in response features to eye cuticle attachments.

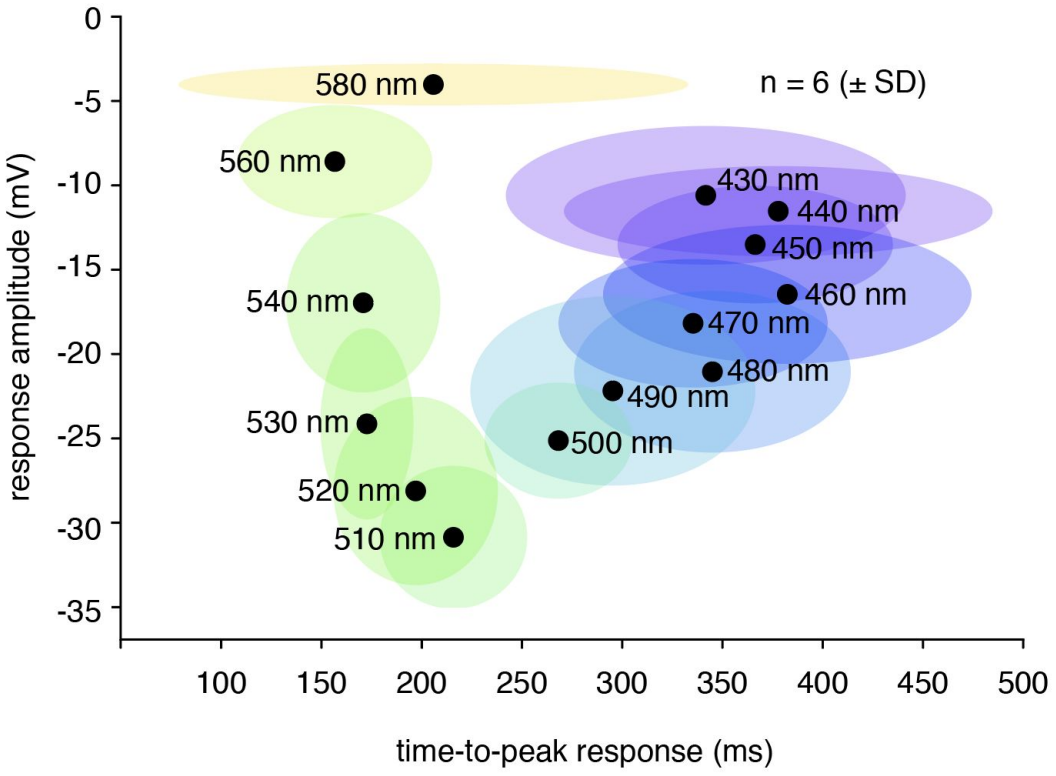

Figure S2. Response amplitude versus time-to-peak for *Acromegalomma vesiculosum* radiolar eye spectral responses in light-off experiments. Data are averaged from the highest-amplitude responding eyes (n = 6), and are shaded with ellipses representing SD and coloured according to human colour perception at each tested wavelength.